JOURNAL OF THEORETICAL AND APPLIED MECHANICS
62, 4, pp. 855-873, Warsaw 2024
https://doi.org/10.15632/jtam-pl/194235

DESIGN METHOD OF DIAMOND BUCKLING RESTRAINED BRACED FRAME STRUCTURE BASED ON NORMAL FORCE BALANCE OF COLUMN JOINTS

Qing Zhang, Ji Yao

Kunming University of Science and Technology, Faculty of Civil Engineering and Mechanics, Kunming, China
e-mail: evanzhangqing@126.com

The diamond buckling restrained braced frame (DBRBF) structure is a novel form of an anti-lateral force support system. A design method for DBRBF structures suitable for various structural types is proposed based on the equilibrium of normal forces in column joints. Taking into account the impact of linear stiffness ratio between upper and lower buckling restrained braced (BRB) elements on the unbalanced forces in column joints of DBRBF sructures, a design method is presented to ensure the normal force balance before and after BRB yield. Building upon this, the calculation method for determining the optimal linear stiffness ratio of two types of BRB elements and the corresponding design method are provided along with the deduced matching conditions for the two types of BRB designs. Furthermore, the relationship between the energy dissipation capacity of BRB elements and deformation of the primary structure under different seismic levels is examined, establishing the condition under which BRB elements serve as the first line of defense prior to yielding of the primary structure. Additionally, the conditions for energy dissipation and ductility guarantee of BRB elements under rare earthquakes are specified. An equation is derived for the length of the working section of BRB elements in DBRBF structures. The results demonstrate that the DBRBF structure can effectively mitigate the adverse effects of BRB elements on the columns through a well-designed approach, enabling realization of matched product designs, and providing a theoretical reference for similar engineering design projects.

Keywords: diamond buckling restrained braced structure, linear stiffness ratio, energy dissipation, design method

1. Introduction

BRB is a type of dissipative element that prevents buckling of the compression steel brace by means of an external restraining mechanism (Yoshino and Karino, 1971; Wakabayashi *et al.*, 1973). It can effectively dissipate energy under both tension and compression. The research has demonstrated that BRB energy dissipation can significantly reduce seismic damage to the primary structure (Di Sarno and Manfredi, 2010). In the structural seismic design, BRBs can enhance the lateral stiffness of the structure, similar to conventional supports, prior to yielding. After yielding, they can undergo plastic deformation to dissipate energy and increase structural damping. Due to its dual functionality of the "bearing" and "energy dissipation", BRB has gained widespread recognition and application once it came out (e.g., Black *et al.*, 2002; Khampanit *et al.*, 2014; among others).

According to the Chinese Seismic Design Code (GB50011-2010, 2010), the primary arrangements for BRB supports include $\wedge$-shaped, $\vee$-shaped, and paired single diagonal bar supports. When the BRB is integrated with the frame structure, the support generates internal force that is transferred through the gusset plate to the beam column joints, potentially causing plastic

hinges. This is particularly evident when the axial force of the support is transferred to concrete members with weak tension, resulting in a more intricate force distribution in the beam column joint area. Altering the connection form or force transfer mode between the gusset plate and the frame is currently a common solution (Benavent-Climent *et al.*, 2015). Furthermore, lateral deformation of the structure leads to compression or tension on the gusset plate due to deformation of the beam and column. This causes stress concentration on the gusset plate, which may lead to premature failure and the subsequent withdrawal of the BRB from operation (Maheri and Ghaffarzadeh, 2008). Simultaneously, the reaction of the gusset plate significantly impacts the beam column joints in an adverse manner. Therefore, several innovative design methods have been proposed to mitigate the negative effects of gusset plates on frame members (Berman and Bruneau, 2009; Lin *et al.*, 2014).

To address the issue of adverse interaction between the brace and structural members, Qu *et al.* (2013, 2015) proposed a zigzag arrangement of BRBs in a reinforced concrete frame, with the removal of reinforced concrete beams in the supporting span. Under lateral deformation, the horizontal force components of adjacent BRBs axial forces counteract each other, effectively mitigating or even eliminating the horizontal force components at the nodes. Additionally, Qu *et al.* (2017) and Xie (2016) introduced a double K-shaped support layout (Fig. 1) as an alternative solution. In this configuration, any two adjacent BRBs always exert opposing forces. At each node, one BRB experiences tension while the other undergoes compression. The resulting normal forces at the node offset each other, thereby reducing the normal unbalanced force and preventing stress concentration in the node plate. Moreover, the BRB node is positioned away from potential "plastic hinges" at the ends of reinforced concrete beams and columns. This ensures that the plastic behavior of the main structural members does not adversely interact with the BRB joints, thus avoiding any detrimental impact on the gusset plates.

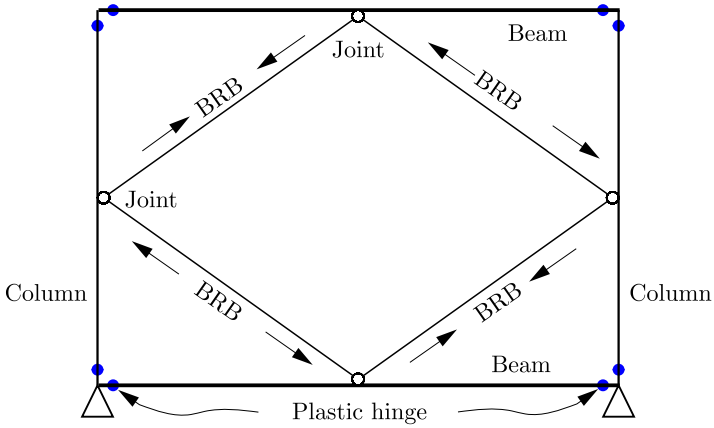

Fig. 1. Reinforced concrete frames braced by BRBs in double-K configuration

In ANSI/AISC 341-02 (2002), a K-braced frame is defined as an OCBF (ordinary concentrically braced frame) with a pair of diagonal braces connected to a single point within the clear height of the column on one side. The definition in ANSI/AISC 341-10 (2010) evolves to describe a braced frame arrangement where the brace is connected to a column with no out of plane brace. Based on these definitions, it is evident that the support structure depicted in Fig. 1 falls under the category of K-bracing. However, the Chinese Seismic Design Code (GB50011-2010, 2010) and ANSI/AISC341-10 (2010) do not recommend the use of K-bracing arrangements for supports. This recommendation also applies to the layout of BRBs due to the adverse effect of the normal unbalanced force on the column caused by the support at the node, which accelerates column failure (Sabelli *et al.*, 2013). In the elastic stage of ordinary steel supports, the normal stress at the beam and column nodes can be offset if the tension and compression members

produce the same strain and stress. In this case, the support only generates an additional axial force on the beam and column. However, as the transverse load and horizontal displacement increase, the compression member will buckle and cease to function. At this point, the brace will induce additional axial force and bending moment on the beam and column, resulting in detrimental effects on the seismic performance of the main structural members.

However, in Japan, there is always the possibility of connecting braces within the uninterrupted span of the column. For instance, Japan proposed the employment of a minimal-intrusion arm damper, which establishes a connection between the midspan of the beam and the upper section of the column. When the damper is activated, it generates a normal shear force on the column, and the magnitude of the detrimental shear force on the column relies on the normal component force generated at the node during energy dissipation of the damper (Kurata *et al.*, 2016). Numerous scholars have conducted valuable investigations on similar matters as well. For instance, Fan *et al.* (2021) examined the rhombic configuration of conventional steel braced steel frame structures. In comparison to the configuration of $\wedge$-shaped and singly inclined bars, they discovered that the rhombic arrangement enhanced redundancy and ductility of the structure. Taking into consideration the adverse effects of unbalanced support forces on the frame beams and columns, they proposed a performance-based seismic design approach for rhombic grid braced frame structures. Qu *et al.* (2017) and (Xie, 2016) conducted an experimental study on the damage mechanism, seismic performance, and mechanical performance of joints of RC frames with double K shaped BRBs. This arrangement effectively enhances the lateral stiffness of the structure and mitigates the shear force on the connection interface of concrete members caused by the braces.

The DBRBF structural system is a novel type of lateral force-resistant BRB supporting structure. It employs a configuration where four BRBs are arranged in a single-story and single--span layout, with their axes combined to form a diamond shape. This arrangement effectively keeps the BRB nodes away from regions with high bending moments, thereby reducing the adverse effects on structural members. Additionally, it enhances the redundancy and ductility of the structure (Fig. 1). Geometrically, each pair of BRBs and columns forms a K-shaped node. However, unlike the K-shaped layout, the diamond-shaped layout has a fixed node position at the midpoint of the column. Consequently, the axial force distribution of the pull rod and the compression rod cannot be adjusted by changing the node position. Nevertheless, the diamond--shaped layout facilitates the achievement of reasonable included angles between the BRBs, beams, and columns, thus providing convenience during construction.

On the other hand, the performance of BRB support differs from that of conventional steel support. BRB has the ability to bear yield due to its ability to continue functioning even after yielding, regardless of tension and compression. As the structure can be seen as a vertical cantilever beam with shear and bending deformation, the structural displacement is a combination of shear and bending deformation. The upper part of the structure is deformed as Δ_1, while the lower part is deformed as Δ_2. Whether the BRB layout is double K or diamond, Δ_1 is not equal to Δ_2 (Fig. 2). Therefore, based on the deformation coordination, the tensile and compressive deformations of the two upper $\wedge$-shaped BRBs are the same, denoted as δ_1, and the two lower $\vee$-shaped BRBs have the same deformation, denoted as δ_2, but δ_1 is not equal to δ_2. In other words, the deformation of BRB is symmetrical from the left to right and from the top to bottom, resulting in a complex stress state of the column node and an unbalanced force of the column node. Thus, according to the Chinese Seismic Design Code (GB50011--2010, 2010) for steel structures, the normal unbalanced force caused by brace buckling should not be considered for frame beams connected with $\wedge$-shaped and $\vee$-shaped BRB braces, and frame columns should not have K-shaped joints. Therefore, in order to eliminate the unbalanced force of column joints caused by bracing in the DBRBF structural system and ensure safety of

columns, solving the problem of column safety is the first and key issue in such a structural design.

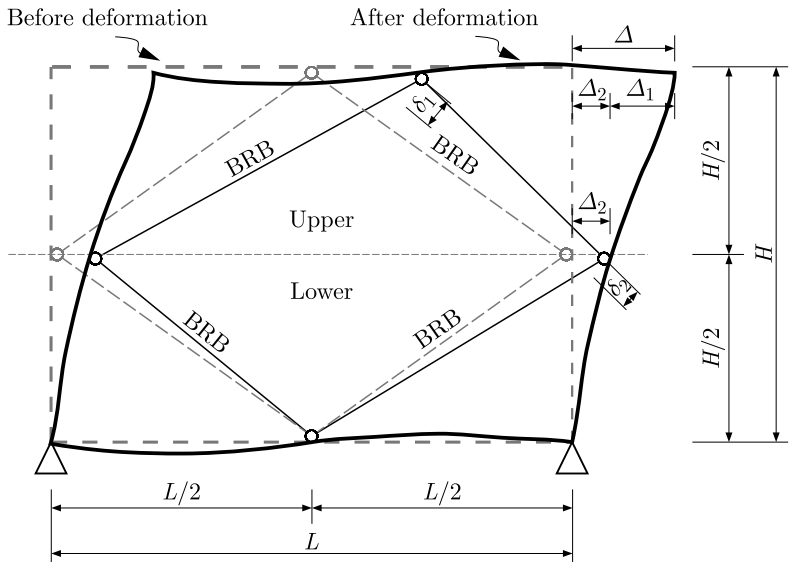

Fig. 2. Deformation of DBRBF structure depicted in a schematic manner

In this paper, the theoretical establishment of the design method for DBRBF is presented, focusing on the geometric configuration characteristics. The adverse effects of the normal unbalanced force of the node on the column are addressed, and the design method for matching BRB products with the structural performance target needs is discussed. The constraints on a BRB product design under different levels of a seismic action are explored, leading to valuable conclusions that facilitate the design of DBRBF. These findings hold significant implications for similar engineering applications.

2. Effect of the BRB linear stiffness ratio on the unbalanced force of DBRBF column joints

Based on the inherent static characteristics of the DBRBF structural system, it exhibits both symmetry and antisymmetry (Fig. 3). From the aforementioned analysis, it can be observed that if the linear stiffness of the upper two BRB_1 braces is equal, and the linear stiffness of the lower two BRB_2 braces is equal, the normal force at the beam node caused by the BRB under horizontal seismic force will naturally equilibrate, effectively nullifying the normal forces at the beam node and exerting no contribution to the column axial force. However, this is not the case for the column joints. If the linear stiffness of BRB_1 and BRB_2 is equal, the axial forces of BRB_1 and BRB_2 will differ in the elastic stage due to the uneven deformation between the upper and lower portions of the structure, resulting in an imbalance of the normal forces at the column joints. It has been proven that conventional design methods, which assume equal BRB linear stiffness in the same layer and span, lead to the same axial internal force values F_1 for the upper two BRB_1 braces and the same axial internal force values F_2 for the lower two BRB_2 braces, but $F_1 \neq F_2$, indicating that the normal force caused by the BRB at the column node cannot be balanced. Consequently, the conventional design method fails to eliminate the adverse effects of unbalanced forces caused by the BRB at the node on the column. Therefore, finding a rational design method that ensures column safety is crucial in the design of the DBRBF structural system.

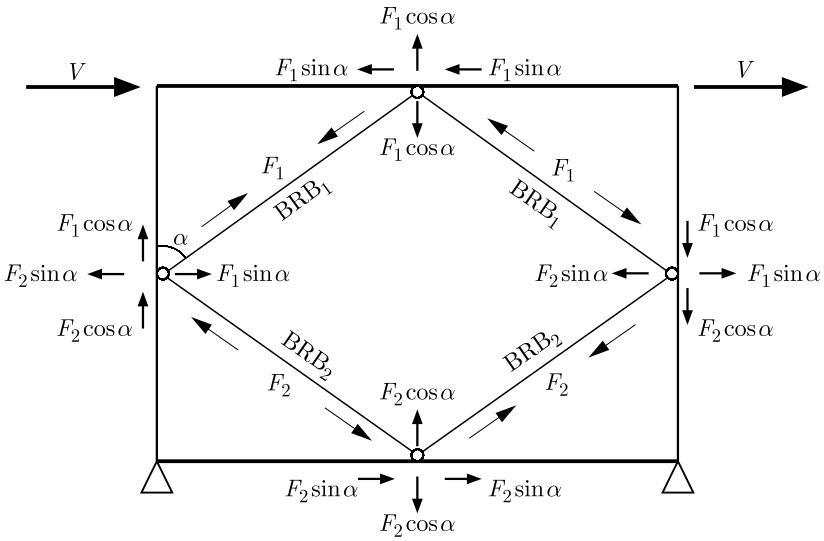

Fig. 3. Equilibrium of internal forces structural model of DBRBF

This paper aims to utilize the approach of adjusting the linear stiffness ratio of BRB_1 and BRB_2 in order to achieve equal axial internal forces among the four BRBs in the elastic stage. The objective is to eliminate the unbalanced force at the column joint prior to BRB yielding. Let K1 represent the linear stiffness of BRB_1 and K2 represent the linear stiffness of BRB_2 and define the linear stiffness ratio K_i as K_1/K_2. To analyze the impact of changes in the linear stiffness ratio on the unbalanced force at column joints caused by BRB internal forces, a frame structure example is examined.

The structure is a single span reinforced concrete frame (DBRBF) shown in Fig. 2. The height of each floor is H=3600mm, with column sections measuring 400 mm×400 mm. The beam span is $L = 4200$ mm, with a section of 200mm×400 mm and C30 concrete. The linear stiffness of BRB_1, denoted as K_1, varies according to different stiffness ratios. On the other hand, the linear stiffness of BRB_2, denoted as K_2, is fixed. The section of BRB_2 is fixed at 30 mm×30 mm, with a vertical force of $V = 200$ kN. By conducting a static analysis of the structure, the variations of BRB_1 and BRB_2 axial internal forces with respect to the linear stiffness ratio K_i are obtained and shown in Fig. 4.

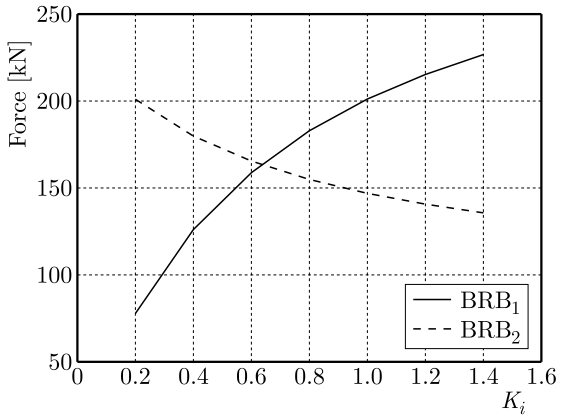

Fig. 4. A diagram of the relationship between the value of the BRB axial force and the linear stiffness ratio K_i

The analysis findings indicate that in the case of a DBRBF structural system, the selection of structural type design (such as storey height, span, section of structural members, material

properties, etc.) greatly influences the internal forces of BRB_1 and BRB_2 when the linear stiffness ratio K_i is changed. There exists a specific linear stiffness ratio (referred to as the optimal linear stiffness ratio K_r) which ensures that the axial forces of BRB_1 and BRB_2 are equal. It has been demonstrated that when $K_i = K_r$, the normal forces at the column nodes cancel each other out, achieving a balance. The larger the deviation between the actual linear stiffness ratio K_i of BRB_1 and BRB_2 and the optimal linear stiffness ratio K_r, the greater the difference in the axial internal forces of BRB_1 and BRB_2, and the more significant the unbalanced force at the column joints. If BRB_1 and BRB_2 have the same linear stiffness ($K_i = 1$), there may be a considerable difference in the axial internal forces between them, and the unbalanced force caused by BRB_1 and BRB_2 at the column joints cannot be neglected.

3. Design method for the normal force balance of column joints

The working performance of BRB can be divided into two stages: the elastic stage and the yield stage. In the elastic stage, when the linear stiffness ratio is K_r, four BRBs exhibit the same bearing capacity F ($F = F_1 = F_2$). The normal forces at the beam and column joints caused by BRB are in equilibrium. Determining the linear stiffness ratio K_r at this stage is a challenging task for engineers. As the lateral deformation of the structure increases, BRBs transition into the yield stage, this is the second stage. Since the linear stiffness of BRB_1 and BRB_2 may differ in the first stage, ensuring that all four BRBs have the same yield bearing capacity and yield simultaneously is also a problem faced by engineers. The next step involves analyzing the two-stage design method of the DBRBF structure separately.

3.1. Normal force balance condition of the column node before BRB yielding

The preceding analysis demonstrates that the DBRBF structural system, with its distinctive geometric characteristics of BRB arrangement and structural deformation properties, can effectively mitigate the unbalanced forces at column joints by adjusting the stiffness ratio of BRB_1 and BRB_2. Consequently, the equilibrium condition of normal forces at the column node during the initial stage can be expressed as

$$K_1 = K_r K_2 \tag{3.1}$$

At its current stage, the BRB is in the elastic phase and exhibits similar working performance to regular supports. The single degree of freedom system of the DBRBF is analyzed using the force method for static analysis. Due to symmetry and antisymmetry of the structure, it is sufficient to analyze only half of the structure, as depicted in Fig. 5. The BRB axes have length of LB, and BRB_1 and BRB_2 have axial tension and compression stiffness values of EA_1 and EA_2, respectively. The linear stiffness values are $K_1 = EA_1/L_B$ and $K_2 = EA_2/L_B$ for BRB_1 and BRB_2, respectively. The bending stiffness of the beam and column are E_1I_1 and E_2I_2, respectively. The beam has a span of L, the structural storey height is H, and α represents the included angle between the BRB and the column. Under the horizontal force V, let X_1 and X_2 be the axial forces generated by BRB_1 and BRB_2, respectively, and X_3 be the reaction force at the beam node. The mechanical equation can then be expressed as

$$\begin{bmatrix} \delta_{11} & \delta_{12} & \delta_{13} \\ \delta_{21} & \delta_{22} & \delta_{23} \\ \delta_{31} & \delta_{32} & \delta_{33} \end{bmatrix} \begin{bmatrix} X_1 \\ X_2 \\ X_3 \end{bmatrix} + \begin{bmatrix} \Delta_{1p} \\ \Delta_{2p} \\ \Delta_{3p} \end{bmatrix} = \mathbf{0} \tag{3.2}$$

One can get Eqs. (3.3) and (3.4) from Fig. 5, according to the Mohr integration method. Due to the relatively small influence of the axial force on deformation of components, in order to

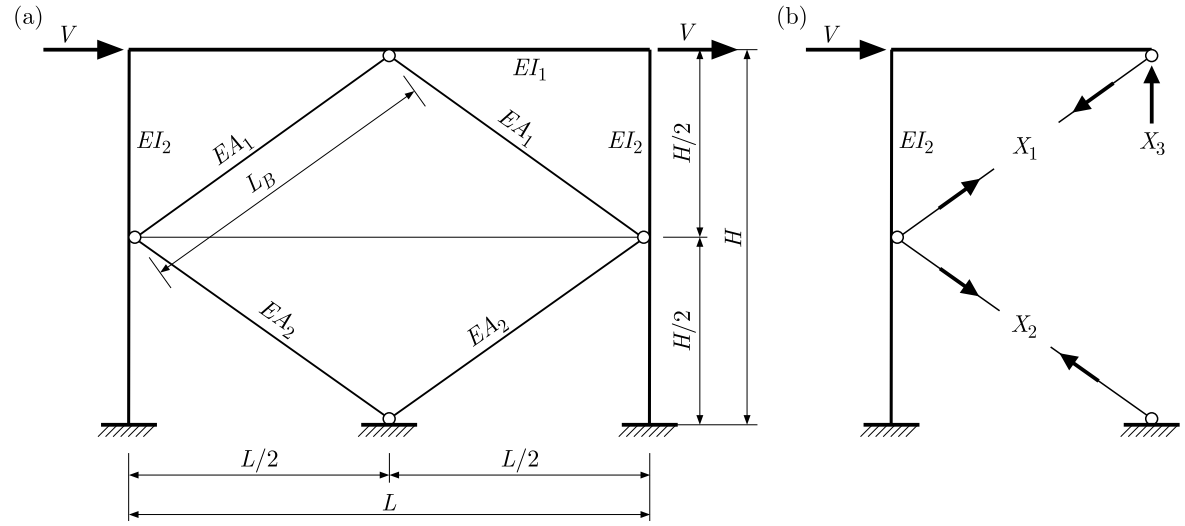

Fig. 5. Structural calculation parameter model of DBRBF: (a) parameter model of the structure, (b) semi structural mechanical model

facilitate calculation, the influence of the axial force on beam column deformation was ignored when deriving the formula

$$\begin{aligned}
&\delta_{11} = \frac{H^3 \sin^2\alpha}{24E_2I_2} + \frac{LH^2\sin^2\alpha}{24E_1I_2} + \frac{\sqrt{L^2+H^2}}{2EA_1} \qquad \delta_{22} = \frac{H^3\sin^2\alpha}{24E_2I_2} + \frac{\sqrt{L^2+H^2}}{2EA_2} \\
&\delta_{33} = \frac{L^3}{24E_1I_1} + \frac{2L^2H}{24E_2I_2} \qquad \delta_{12} = \delta_{21} = 0 \\
&\delta_{13} = \delta_{31} = -\frac{L^2H\sin\alpha}{24E_1I_1} - \frac{LH^2\sin\alpha}{16E_2I_2} \qquad \delta_{23} = \delta_{32} = -\frac{LH^2\sin\alpha}{16E_2I_2}
\end{aligned} \tag{3.3}$$

and

$$\Delta_{1p} = \frac{VH^3\sin\alpha}{48E_2I_2} \qquad \Delta_{2p} = \frac{5VH^3\sin\alpha}{48E_2I_2} \qquad \Delta_{3p} = -\frac{VLH^2}{4E_2I_2} \tag{3.4}$$

Solve Eq. (3.2) to get

$$\begin{aligned}
X_1 &= -\frac{\Delta_{1p}\delta_{23}^2 - \Delta_{2p}\delta_{13}\delta_{23} + \Delta_{3p}\delta_{13}\delta_{22} - \Delta_{1p}\delta_{22}\delta_{33}}{\delta_{22}\delta_{13}^2 + \delta_{11}\delta_{23}^2 - \delta_{11}\delta_{22}\delta_{33}} \\
X_2 &= -\frac{\Delta_{2p}\delta_{13}^2 - \Delta_{1p}\delta_{13}\delta_{23} + \Delta_{3p}\delta_{13}\delta_{11} - \Delta_{2p}\delta_{11}\delta_{33}}{\delta_{22}\delta_{13}^2 + \delta_{11}\delta_{23}^2 - \delta_{11}\delta_{22}\delta_{33}} \\
X_3 &= -\frac{\Delta_{1p}\delta_{13}\delta_{22} + \Delta_{2p}\delta_{11}\delta_{23} - \Delta_{3p}\delta_{11}\delta_{22}}{\delta_{22}\delta_{13}^2 + \delta_{11}\delta_{23}^2 - \delta_{11}\delta_{22}\delta_{33}}
\end{aligned} \tag{3.5}$$

To counteract the imbalanced forces at the joints, it is necessary to determine the internal forces $X_1 = X_2$ for BRB_1 and BRB_2, which can be obtained from Eqs. (3.5)

$$\begin{aligned}
&\Delta_{1p}\delta_{23}^2 - \Delta_{2p}\delta_{13}\delta_{23} + \Delta_{3p}\delta_{13}\delta_{22} - \Delta_{1p}\delta_{22}\delta_{33} \\
&\quad = -(\Delta_{2p}\delta_{13}^2 - \Delta_{1p}\delta_{13}\delta_{23} + \Delta_{3p}\delta_{13}\delta_{11} - \Delta_{2p}\delta_{11}\delta_{33})
\end{aligned} \tag{3.6}$$

By substituting Eqs. (3.2) and (3.4) into Eq. (3.6), we can derive

$$\frac{1}{EA_1}\Big(\frac{5\tan\alpha}{3E_1I_1} + \frac{4}{E_2I_2}\Big) - \frac{1}{EA_2}\Big(\frac{11\tan\alpha}{3E_1I_1} + \frac{4}{E_2I_2}\Big) = 0 \tag{3.7}$$

Hence, the optimal linear stiffness ratio for the single degree of freedom systems BRB_1 and BRB_2 can be expressed as

$$K_r = \frac{EA_1/L_B}{EA_2/L_B} = \frac{5E_2I_2\tan\alpha + 12E_1I_1}{11E_2I_2\tan\alpha + 12E_1I_1} \tag{3.8}$$

If the DBRBF structural system employs a steel or reinforced concrete beam and a column with the same grade of concrete, the simplified equation can be denoted as

$$K_r = \frac{K_1}{K_2} = \frac{5I_2\tan\alpha + 12I_1}{11I_2\tan\alpha + 12I_1} \tag{3.9}$$

In Eq. (3.9), $\tan\alpha$ represents the ratio of the structural span to the storey height, denoted as L/H. Equation (3.8) demonstrates that the optimal linear stiffness ratio of the DBRBF structural system BRB_1 and BRB_2 is determined by the inherent properties of the structure, relying on its unique geometric characteristics and the bending stiffness of its structural members. This ratio is unaffected by the horizontal force and is solely influenced by the three parameters: E_1I_1, E_2I_2, and α. This characteristic facilitates the simplified calculation of the DBRBF structural system analysis. Once the structural type selection is determined for a project, the optimal stiffness ratio of BRB_1 and BRB_2 in DBRBF structures remains a fixed value. Under predefined structural layout conditions, the bending stiffness of the beams and columns becomes the decisive factor for modifying the optimal linear stiffness ratio K_r. This feature can be utilized to develop programs that calculate the optimal linear stiffness ratio for multi-degree of freedom systems and continuous beams.

The recommended range of the included angle α between the BRBs and the column, as suggested by The Code for Seismic Design of Buildings (GB50011-2010, 2010), is 35°-55°. However, in this study, the included angle α is appropriately increased to 22.5°-67.5° ($\pi/8$ $3\pi/8$). From Fig. 6, it can be observed that for the DBRBF structure, under the same bending stiffness ratio of the beam and column, the optimal linear stiffness ratio K_r decreases as the included angle α increases. Conversely, when the geometric characteristics of the structural layout are

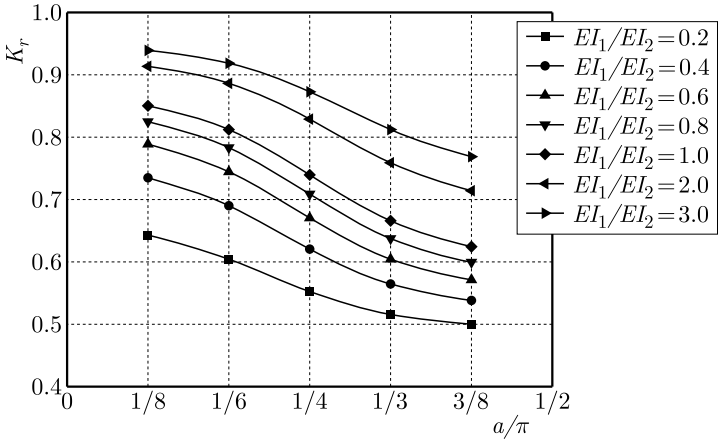

Fig. 6. Optimal linear stiffness ratio curve for different angles α

determined, with the same included angle α, the optimal linear stiffness ratio K_r increases with an increase in the bending stiffness ratio of the beam to the column. In the engineering design process, the structural system can be adjusted comprehensively based on the aforementioned change rules. Considering the recommended range of the included angle α in the specification and the requirement for strong columns and weak beams, the common range of the optimal linear stiffness ratio K_r in actual projects is 0.55-0.75. It has been demonstrated that although the axial force values of the four BRBs can be equalized by adjusting the stiffness ratio, the stiffness

of BRB_1 and BRB_2 are not equal due to the inherent properties of the DBRBF structure. Hence, in addition to the usual equivalent design based on calculation parameters, the design of BRB products also needs to consider matching the performance of BRB_1 and BRB_2 products. This ensures that BRB_1 and BRB_2 can have the same yield bearing capacity and meet structural deformation characteristics under different stiffness conditions.

3.2. Normal force balance conditions of column joints after BRB yielding

Due to inadequate capability of mainstream design software in China (e.g. YJK, PKPM) to accurately simulate the mechanical behavior of BRBs and node domains, the design software typically substitutes their mechanical behavior with two-force bars and achieves product design through parameter equivalence. The key parameters of the product mainly encompass axial stiffness, yield bearing capacity, yield displacement, and post-yield stiffness. Based on the previous analysis, it is observed that, under the optimal linear stiffness ratio K_r, BRB_1 and BRB_2 exhibit the same bearing capacity but different linear stiffness in the first stage of the DBRBF structure. Consequently, the separate and arbitrary equivalence design of BRB_1 and BRB_2 products is not viable. This approach may lead to mismatched mechanical behavior, such as yield bearing capacity and yield displacement between BRB_1 and BRB_2 in the second stage, resulting in unbalanced forces at the column joint. Therefore, in order to ensure that BRB_1 and BRB_2 possess equivalent bearing capacity after yielding and yield simultaneously, it is imperative to conduct performance matching design for major equivalent parameters, including the yield force and yield displacement of BRB_1 and BRB_2 products.

The primary focus of this paper is to examine the design of performance matching for BRB_1 and BRB_2 products. To simplify the analysis, the mechanical behavior of the BRB is divided into three parts: the energy dissipation section and two connection sections. The energy dissipation section has a length of L_e and a section area of A_e. The connection section has a length of L_j and an equivalent section area of A_j, as illustrated in Fig. 7. The connection section comprises various elements such as concrete components, gusset plates, core material elastic sections, and transition sections. It has been demonstrated that the actual length, stiffness, and cross-sectional area of BRB products differ from those of the two-force bar, but they exhibit equivalent performance during operation.

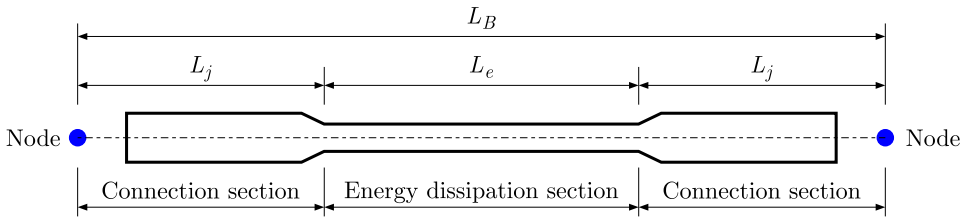

Fig. 7. BRB axial series composition

LY100, LY160, LY195, LY225, Q235, Q345, Q390, etc. are commonly utilized materials in the energy dissipation section of BRB (Buckling Restrained Brace) in Chinese projects. When designing BRB products, designers have some flexibility in selecting different steel yield strengths to determine the appropriate section area for the energy dissipation section and the individual areas of each part in the connecting section. Subsequently, they can adjust the lengths of the energy dissipation section and each part of the connecting section to achieve equivalence with the design parameters of a two-bar system. This ensures the mechanical behavior equivalence. Therefore, the design of a single BRB product results in various BRB products with different core materials that are equivalent to the same two-bar parameters (Wu *et al.*, 2021).

The results depicted in Fig. 7 exhibit that the linear stiffness of BRB products can be represented as

$$\frac{1}{K} = \frac{1}{K_e} + \frac{2}{K_j} \tag{3.10}$$

In Eq. (3.10), K represents the equivalent linear stiffness of the axis as calculated by BRB. K_e and K_j, on the other hand, refer to the linear stiffness of the energy dissipation section and the equivalent stiffness of the connection section, respectively

$$K_{ie} = \frac{EA_{ie}}{L_{ie}} \qquad K_{ij} = \frac{EA_{ij}}{L_{ij}} \qquad i = 1, 2 \tag{3.11}$$

By substituting Eq. (3.11) and $K = EA/L_B$ into Eq. (3.10), we can derive the ratio of the core section area to the core section length for both BRB_1 and BRB_2

$$\frac{A_{1e}}{L_{1e}} = \frac{1}{L_B - 2L_{1j}\frac{A_1}{A_{1j}}} A_1 \qquad \frac{A_{2e}}{L_{2e}} = \frac{1}{(L_B - 2L_{2j}\frac{A_2}{A_{2j}}} A_2 \tag{3.12}$$

The BRB yield bearing capacity F_y is

$$F_y = \sigma_y A_e = \eta f_y A_e \tag{3.13}$$

The parameter η represents the coefficient of super strength in the core energy dissipation section of steel, which is incorporated to account for the Bauschinger effect (as shown in Table 1).

Table 1. The Bauschinger coefficient

Steel	LY100	LY160	LY195	LY225	Q235	Q345	Q390
η	1.1	1.1	1.15	1.1	1.25	1.1	1.05

When both BRB_1 and BRB_2 exhibit an equal yield strength capacity F_y, then

$$F_y = \eta_1 f_{1y} A_{1e} = \eta_2 f_{2y} A_{2e} \tag{3.14}$$

By substituting Eq. (3.14) into Eqs. (3.12), the equilibrium condition of the normal force in the column node can be derived when the BRB reaches its yield point simultaneously

$$\frac{L_{1e}}{L_{2e}} = \frac{\beta}{K_r} \frac{L_B - 2L_{1j}\frac{A_1}{A_{1j}}}{L_B - 2L_{2j}\frac{A_2}{A_{2j}}} \tag{3.15}$$

Let β represent the yield strength ratio of the energy dissipation section steel of BRB_1 and BRB_2

$$\beta = \frac{\eta_2 f_{2y}}{\eta_1 f_{1y}} \tag{3.16}$$

Utilizing the steel strength data provided in Table 1, the yield strength ratio β of the energy dissipation section can be calculated using Eq. (3.16). The range of β has been demonstrated to be between 0.27 and 3.72. By selecting different types of steel to adjust the linear stiffness of both the core material energy dissipation section and the connecting section, it is possible to ensure that the yield forces of BRB_1 and BRB_2 are equal. Moreover, there is ample flexibility in terms of the matching space when different linear stiffness values are employed.

Equation (3.15) demonstrates that the design of the energy dissipation section of the core material in BRB_1 and BRB_2 products is mutually constrained under the double constraints of

maintaining the same optimal stiffness ratio in the first stage and the same yield force in the second stage. The length and linear stiffness of the energy dissipation section in either BRB_1 or BRB_2 product must correspond to the length and linear stiffness of the energy dissipation section in the other product. Additionally, this matching relationship is influenced by the material properties and the linear stiffness of the connection section selected for both products. When this criterion is satisfied, BRB_1 and BRB_2 will have the same yield force and can yield simultaneously, thereby achieving a balanced normal force at the column node after BRB yielding. In the project, the design of BRB_1 can be carried out initially based on the fundamental performance parameters of both BRB_1 and BRB_2, followed by the design of BRB_2 using the basic performance parameters of BRB_2 and Eq. (3.15). Conversely, BRB_2 can be designed first, and then BRB_1 can be designed according to Eq. (3.15).

4. The BRB products are reasonably matched with the performance objectives of the main structure

In the field of structural design, the storey displacement angle is a crucial performance indicator for a structure. Its limit value is dependent on the type of structure and the performance level of the structure. For structures of the same type, the inter-story displacement angle limit is a fixed value. When compared to commonly used layout forms such as a single diagonal brace, $\wedge$-shaped brace, and $\vee$-shaped brace, the diamond layout form BRB exhibits the minimum axial deformation. During an earthquake, BRB functions as an energy dissipation member and should enter the yielding energy dissipation state before the main structure, serving as the primary line of defense against a seismic activity. Additionally, BRB must possess sufficient ductility safety reserves, allowing it to operate without damage during rare earthquakes. In engineering design, the performance parameters of BRB products are established based on the performance objectives of the structure. The performance level at which BRB enters the yield energy dissipation state is determined by the compatibility between the product performance parameters and the performance objectives of the structure. This relationship directly impacts the rationality of the design results. This paper proposes a method for rational matching of product performance parameters and structure performance objectives, in accordance with the requirements of BRB product performance parameters for main structure performance objectives.

4.1. BRB as the control condition of the first seismic fortification line of the structure

The calculation diagram for lateral deformation of the DBRBF structural system when subjected to horizontal forces is shown in Fig. 8.

In Fig. 8, Δ represents the horizontal displacement between floors in the frame structure, while Δ_1 and Δ_2, respectively, denote the horizontal inter-story displacements of the upper and lower halves of the structure. θ represents the angular displacement of the structure between floors. When the structure experiences lateral deformation, the axial deformations δ_1 and δ_2 of BRB_1 and BRB_2 can be calculated using

$$\delta_1 = \frac{F}{EA_1} L_B \qquad \delta_2 = \frac{F}{EA_2} L_B \tag{4.1}$$

By taking into account the constraint of the optimal linear stiffness ratio, we can derive

$$\delta_1 = \frac{1}{K_r} \delta_2 \tag{4.2}$$

The horizontal displacement between the top and bottom of the column Δ can be defined as the difference in the horizontal displacement between the upper half layer Δ_1 and the lower half layer Δ_2. As θ is a small angle, so $\tan\theta \approx \theta$

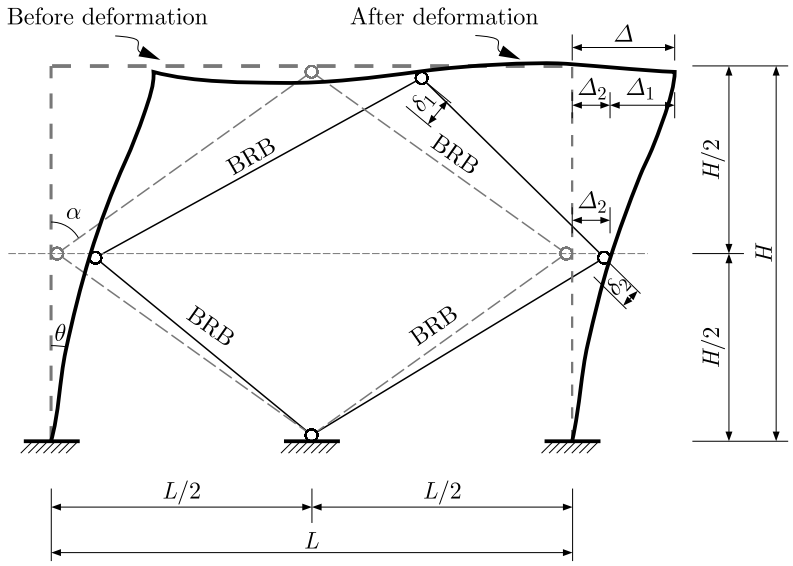

Fig. 8. Schematic of DBRBF structure deformation calculation

$$\Delta = \Delta_1 + \Delta_2 = \frac{\delta_1}{\sin\alpha} + \frac{\delta_2}{\sin\alpha} = H\tan\theta = H\theta \tag{4.3}$$

By substituting $L = H/2\cos\alpha$, Eq. (3.11), Eq. (4.1), and Eq. (4.2) into Eq. (4.3), we can derive

$$\theta = \frac{K_r+1}{\sin 2\alpha}\frac{A_{1e}}{A_1}\varepsilon_{1e} = \frac{K_r+1}{K_r\sin 2\alpha}\frac{A_{2e}}{A_2}\varepsilon_{2e} \tag{4.4}$$

Let ε_{1e}, ε_{2e} be the strain of the core material energy dissipation sections of BRB_1 and BRB_2, respectively. Upon yielding of BRB, the strain $\vee$ of the energy dissipation section is obtained, and the corresponding interlayer displacement angle of the DBRBF structure when BRB yields is given by

$$\theta_{By} = \frac{K_r+1}{\sin 2\alpha}\frac{A_{1e}}{A_1}\varepsilon_{1ey} = \frac{K_r+1}{K_r\sin 2\alpha}\frac{A_{2e}}{A_2}\varepsilon_{2ey} \tag{4.5}$$

To activate the energy dissipation of BRB before the main frame in the DBRBF structure, it is required that the inter-story displacement angle θ_{By} is smaller than the inter-story displacement angle θ_y when the structure reaches its yield point

$$\theta_{By} < \theta_y \tag{4.6}$$

4.2. BRB matching design under different performance levels

According to literature (Li *et al.*, 2010), BRB can be categorized into three types in engineering applications based on different stages of energy dissipation: damper type, energy dissipation type, and bearing type. The damper type BRB functions as a damper, dissipating energy during frequent earthquakes. The energy dissipating BRB maintains elasticity and only offers stiffness under frequent earthquakes, but yields to dissipate energy during fortification earthquakes or rare earthquakes. The load-bearing BRB remains elastic at all levels and solely provides stiffness. It has been demonstrated that the level at which BRB enters the energy dissipation state significantly impacts the structural design. Therefore, the selection of material yield strength and adjustment of the energy dissipation section length L_e of BRB to align with the performance target of the structure under varying levels of the seismic action is a crucial aspect in the design of the DBRBF structural system. Currently, the availability of steel grades for BRB products is

limited, making it important to determine the appropriate material yield strength and L_e length for achieving the desired working performance target.

As depicted in Fig. 7 above, the axial deformation of the Buckling-Restrained Brace (BRB) is characterized by deformation of the energy dissipation section δ_e and deformation of the connecting section δ_j

$$\delta = \delta_e + \delta_j = \varepsilon_e L_e + 2\varepsilon_j L_j \tag{4.7}$$

Let ε_e and ε_j denote the strain of the energy dissipation section and the connecting section, respectively. A previous research (Cai *et al.*, 2005) indicates that the ratio of the strain in the connecting section to the total axial strain of the BRB is less than 6%. This is primarily due to the requirement in BRB product design that the connecting section should remain elastic even when the yield section of the BRB experiences strain strengthening or failure caused by earthquakes at different levels. Consequently, the deformation of the connecting section can be disregarded, and the strain in the energy dissipation section can be approximately considered as the axial strain

$$\delta_1 = \varepsilon_{1e} L_{1e} \qquad \delta_2 = \varepsilon_{2e} L_{2e} \tag{4.8}$$

The determination of the BRB deformation and structural displacement angle θ in any state can be achieved by substituting Eqs. (4.8) and (4.2) into Eq. (4.3)

$$\theta = \frac{(1+K_r)\varepsilon_{1e} L_{1e}}{H \sin\alpha} = \frac{(1+K_r)\varepsilon_{2e} L_{2e}}{K_r H \sin\alpha} \tag{4.9}$$

Definition λ represents the ratio of length of the energy dissipation section of the BRB to overall length of its axis, denoted as $\lambda = L_e/L_B$. It is evident that λ is less than 1. Eq. (4.10) is derived from Eq. (4.9)

$$\theta = \frac{(1+K_r)\varepsilon_{1e} \lambda_1}{\sin 2\alpha} = \frac{(1+K_r)\varepsilon_{2e} \lambda_2}{K_r \sin 2\alpha} \tag{4.10}$$

The response of BRB_1 and BRB_2 subjected to the specific horizontal seismic loading is represented by

$$\varepsilon_{1e} = \frac{\theta_i \sin 2\alpha}{(1+K_r)\lambda_1} \qquad \varepsilon_{2e} = \frac{\theta_i K_r \sin 2\alpha}{(1+K_r)\lambda_2} \tag{4.11}$$

θ_i $(i = 1, 2, 3)$, representing frequent earthquake, fortification earthquake, and rare earthquake, respectively, refers to the angular displacement of the structural storey caused by earthquakes of varying magnitudes. Equation (4.12) describes the conditions for yield energy dissipation of BRB_1 and BRB_2 when subjected to a specific level of earthquake

$$\varepsilon_{1e} = \frac{\theta_i \sin 2\alpha}{(1+K_r)\lambda_1} \geqslant \varepsilon_{1ey} = \frac{\sigma_{1y}}{E} \qquad \varepsilon_{2e} = \frac{\theta_i K_r \sin 2\alpha}{(1+K_r)\lambda_2} \leqslant \varepsilon_{2ey} = \frac{\sigma_{2y}}{E} \tag{4.12}$$

The lengths of the energy dissipation sections of BRB_1 and BRB_2 should satisfy the following conditions when BRB yield energy is consumed at various levels of seismic activity

$$\lambda_1 \leqslant [\lambda_{1i}] = \frac{\theta_i E \sin 2\alpha}{(1+K_r)\sigma_{1y}} \qquad \lambda_2 \leqslant [\lambda_{2i}] = \frac{K_r \theta_i E \sin 2\alpha}{(1+K_r)\sigma_{2y}} \tag{4.13}$$

where $[\lambda_{1i}]$ and $[\lambda_{2i}]$ represent the permissible values for the respective lengths of the energy dissipation sections under the influence of BRB_1 and BRB_2 earthquakes at different intensities. They also denote the maximum lengths of the energy dissipation sections when BRB_1 and BRB_2

reach the state of energy consumption during the occurrence of earthquakes of corresponding intensities.

From Eq. (4.12), it has been demonstrated that an increase in the permissible value of the energy dissipation section length leads to enhanced yield energy dissipation of the BRB under the influence of earthquakes at corresponding levels. Conversely, a decrease in the permissible value of the energy dissipation section length results in shorter energy dissipation section length, which may lead to inadequate ductility reserve of the BRB during rare earthquake events, making it highly susceptible to reaching the limit deformation and experiencing fracture failure. It is also evident that the permissible percentage of BRB energy dissipation section length $[\lambda_i]$ and the material yield strength σ_y are dependent on the performance level target established for the structure. Moreover, the optimal stiffness ratio K_r and the BRB are influenced by the column angle α. Based on the above analysis, it can be concluded that the optimal linear stiffness ratio K_r is associated with the bending stiffness E_1I_1, E_2I_2 and the included angle α of the beam and column making it analogous to the allowable proportion of the energy dissipation section $[\lambda_i]$. This value is solely determined by the four parameters σ_y, E_1I_1, E_2I_2 and α.

In the design of BRB, the proportion of energy dissipation section length should be as large as possible. Too short energy dissipation section length will limit the energy consuming capacity of BRB on the one hand, and deformation of the energy dissipation section will be too large under a rare earthquake on the other hand. When the axial strain of BRB energy dissipation section is less than 3%, BRB can maintain stable mechanical behavior. When the axial strain exceeds 3%, the amplitude of friction on the compression side increases rapidly, and the compression side of the hysteresis curve is prone to instability and buckling failure (Iwata and Murai, 2006). Therefore, the reference (T/CECS817-2021, 2021) stipulates that the length of the energy dissipation section shall not be less than 60% of the total length of the BRB, and the axial strain of the energy dissipation section under the design displacement shall not exceed 3%. As the limit value of structural displacement angle under the action of a fortification earthquake is not clearly specified in the Chinese Code for Seismic Design of Buildings (GB50011--2010, 2010), designers often pay more attention to structural deformation characteristics under frequent and rare earthquakes. Taking the reinforced concrete frame structure as an example, the yield energy dissipation of BRB_1 and BRB_2 under frequent earthquakes and their ductility requirements under rare earthquakes are discussed below.

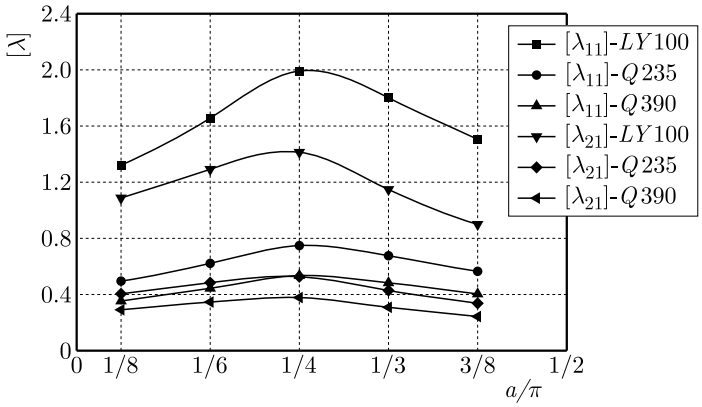

Fig. 9. Curve of $[\lambda]$ for different angles α

In Fig. 9, the fixed $E_1I_1/E_2I_2 = 1.0$ DBRBF concrete frame structure is shown under frequent earthquakes ($\theta 1 = 1/550$). The allowable values for the energy dissipation section percentages of phase BRB_1 and BRB_2, denoted as $[\lambda_{11}]$ and $[\lambda_{21}]$, are displayed in the figure. It can be observed that when other conditions are held constant and the included angle between the BRB and the column is $\alpha = \pi/4$, both BRB_1 and BRB_2 are most likely to experience yield

energy dissipation during frequent earthquakes. Under the same included angle condition, BRB_1 exhibits a higher likelihood of yielding and dissipating energy compared to BRB_2 when utilizing steel with the same yield point in the energy dissipation section.

Figure 10 illustrates the permissible values of length ratios $[\lambda_{11}]$ and $[\lambda_{21}]$ for the energy dissipation sections of BRB_1 and BRB_2 in frequent earthquakes at the optimal angle of $\alpha = \pi/4$. As λ is always less than 1, it can be inferred that the energy consumption requirements of frequent earthquakes are naturally fulfilled when $\lambda > 1$. It is evident from Fig. 10 that only LY100 steel satisfies the yield energy consumption performance target for BRB_1 and BRB_2 under frequent earthquakes. Furthermore, the figure indicates that in the design of BRB_1 and BRB_2 products, choosing steel with a lower yield point for the energy dissipation section facilitates easier yielding and energy consumption in frequent earthquakes. Conversely, higher yield point steel poses challenges in achieving the BRB energy consumption target in frequent earthquakes, with potential difficulty in meeting the requirements stated in document (T/CECS817-2021, 2021). As a result, low yield point steel should be preferred in the product design. Additionally, under the same yield strength of steel, a higher bending stiffness ratio E_1I_1/E_2I_2 between the beam and column leads to a greater proportion of energy dissipation section length for BRB_1 and a smaller limit value of $[\lambda_{11}]$. Consequently, this unfavorably impacts energy consumption of BRB_1 in frequent earthquakes. Conversely, BRB_2 exhibits the opposite trend. Thus, when selecting the structure, a comprehensive consideration of these factors is necessary.

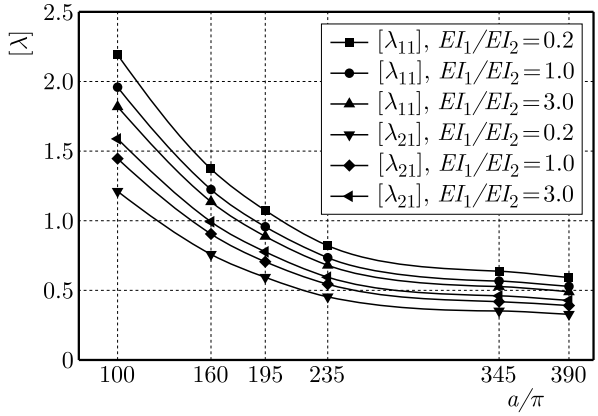

Fig. 10. Curve of $[\lambda]$ for different yield strengths of steel

The analysis above is based on the performance target of frequent earthquakes. Likewise, when determining the design for the DBRBF structure type selection under the influence of fortification earthquakes and rare earthquakes, the allowable values $[\lambda_{1i}]$ and $[\lambda_{2i}]$ for the proportion of the BRB_1 and BRB_2 energy dissipation sections lengths can be obtained by substituting the displacement angle limit value under the corresponding level earthquake into Eq. (4.13). This allows for selection of appropriate steel to achieve the desired yield energy consumption during the fortification earthquake or rare earthquake stage. It has been demonstrated that the DBRBF structural system initiates the yield energy dissipation of the BRB at a specific performance target level. The design of the energy dissipation section is crucial. By considering the structural performance target, geometric characteristics of the structure, and the bending stiffness of the beam and column, the selection of suitable steel should be made to ensure the desired performance of the BRB_1 and BRB_2 products.

4.3. BRB ductility guarantee conditions

The BRB should have a sufficient safety reserve of ductility during rare earthquakes, and also provide enough ductility allowance under the maximum limit of structural elastoplastic

deformation. The previous analysis has shown that length of the energy dissipation section in a diamond-shaped layout for BRBs is shorter compared to the traditional layout. However, a too short energy dissipation section during rare earthquakes can result in a insufficient safety reserve for ductility and potential fracture failure. According to FEMA450 regulation (FEMA450, 2000), the design deformation of BRB products should be determined as 1.5 times the maximum interlayer design deformation. In this study, the axial strain, Eq. (4.14) of the energy dissipation section should not exceed 3% to ensure the ductility of the BRB, as stated in Eq. (4.11)

$$\varepsilon_{1e} = \frac{1.5\theta_3 \sin 2\alpha}{(1+K_r)\lambda_1} \leqslant 3\% \qquad \varepsilon_{2e} = \frac{1.5\theta_3 K_r \sin 2\alpha}{(1+K_r)\lambda_2} \leqslant 3\% \tag{4.14}$$

Further

$$\lambda_1 \geqslant [\xi_1] = \frac{50\theta_3 \sin 2\alpha}{1+K_r} \qquad \lambda_2 \leqslant [\xi_2] = \frac{50\theta_3 K_r \sin 2\alpha}{1+K_r} \tag{4.15}$$

According to Eq. (4.15), the minimum limit proportion of energy dissipation sections BRB_1 and BRB_2, denoted as $[\xi_1]$ and $[\xi_2]$, respectively, is required to meet the ductility requirements in rare earthquakes. The formula shows that the minimum value of the energy dissipation section proportion is only influenced by three parameters E_1I_1, E_2I_2 and α. This dependency is due to K_r being related solely to these three parameters, and not affected by the yield strength of steel used in the energy dissipation section. This differs from the starting condition of BRB yield energy dissipation. The main reason is that the axial strain of the energy dissipation section is set as 3% under rare earthquake conditions. Essentially, the minimum limit of the length proportion of the energy dissipation section is determined by the type of structure, with the minimum length of the BRB energy dissipation section meeting the ductility requirement under rare earthquake action being fixed.

The change curve of the minimum limit $[\xi_1]$ and $[\xi_2]$ of the proportion of energy dissipation section length of BRB_1 and BRB_2 in the DBRBF reinforced concrete frame structure is shown in Fig. 11 for rare earthquakes $\theta_3 = 1/50$. It can be observed from Fig. 11 that when the included angle between the BRB and column is $\alpha = \pi/4$, the proportion of BRB_1 or BRB_2 to the energy dissipation section under a rare earthquake action has the most stringent minimum limit λ. In terms of the proportion of energy dissipation section length under the same included angle,

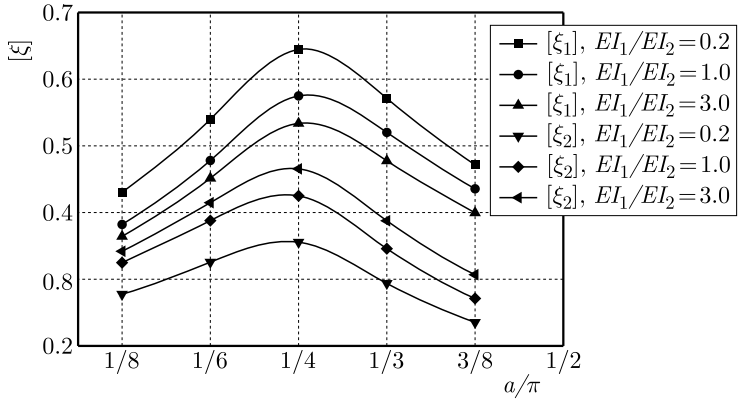

Fig. 11. Curve of $[\xi]$ for different angles α

BRB_1 has higher requirements than BRB_2. Comparing the proportion of energy dissipation section in frequent earthquakes, it can be seen from the maximum limit of λ that the proportion of BRB energy dissipation section under frequent earthquakes has a greater allowable value, indicating a stricter minimum length limit of the energy dissipation section length under the rare earthquake action. This is mainly because the BRB enters the yield energy dissipation state

earlier under rare earthquakes, leading to greater plastic deformation and requiring longer length of the energy dissipation section to ensure ductility.

The previous analysis demonstrates that BRB_1 and BRB_2 products should be designed to both absorb and dissipate energy during corresponding-level earthquakes. They should also ensure that no fractures occur during rare earthquakes, while maintaining a certain level of ductility safety reserve. Therefore, based on the aforementioned analysis, it can be concluded that Eq. (4.16) determines the range of percentage for the energy dissipation sections of BRB_1 and BRB_2 in DBRBF structures

$$[\xi_1] \leqslant \lambda_1 \leqslant [\lambda_1] \qquad [\xi_2] \leqslant \lambda_1 \leqslant [\lambda_1] \tag{4.16}$$

After comparing the calculation formulas on each side of the inequality, it has been demonstrated that the left-hand side of Eqs. (4.16) is a constant value for the given structural type, while the right-hand side is influenced by factors such as material properties, structural selection, and performance objectives. Among these factors, the strength of the core material has a significant impact. As the strength of the core material increases, the calculated value on the right-hand side of Eqs. (4.16) gradually decreases, sometimes even becoming smaller than the left-hand side. As shown in Figs. 10 and 11, BRB starts to consume energy during frequent earthquakes. In the case of DBRBF reinforced frame structures, when LY100 steel is used as the core material, Eqs. (4.16) can be satisfied under any conditions. However, when high-strength steel Q390 is utilized, neither BRB_1 nor BRB_2 can meet the requirements of Eqs. (4.16). This is primarily due to the limitations imposed by λ in completing the product design, making it impossible to achieve energy dissipation during frequent earthquakes while ensuring the ductility safety reserve demand of BRB under rare earthquakes. Thus, it is evident that Eqs. (4.16) is not universally applicable, indicating that BRB_1 and BRB_2 can only fulfill either the energy dissipation condition or the ductility guarantee condition. The interplay between the performance of BRB_1 and BRB_2 leads to a more complex process of core material matching and selection during product design.

The project adopts the DBRBF structural design method, which involves selecting the appropriate structure and calculating the optimal stiffness ratio of BRB_1 and BRB_2. After completing the structural analysis, the performance parameters of BRB_1 and BRB_2 products are obtained. The product design is then carried out based on the requirements of these performance parameters. When designing BRB_1 and BRB_2 products, several conditions need to be considered, including product stiffness matching, post yield strength, deformation matching, as well as startup energy consumption and ductility guarantee conditions, which act as the primary control factors. If the BRB product design fails to meet the performance target requirements, it is necessary to re-optimize the structural design.

The above design methods can be applied to various types of structures, including steel structures, reinforced concrete frame structures with seismic walls, slab column seismic walls, frame core tubes, tubes in tubes, and other structural forms.

5. Conclusion

By adjusting the stiffness ratio of BRB_1 and BRB_2, the adverse effects of brace arrangement on columns can be eliminated, thus achieving a normal force balance of column joints in the elastic stage in the design of the DBRBF structure.

In the design process of BRB_1 and BRB_2 products, achieving a normal force balance at any level stage of column joints relies on parameter matching between the two products, in addition to the conventional design method of BRB product parameter equivalence.

Compared to the traditional BRB layout, the diamond layout exhibits reduced axial deformation and strain in the energy dissipation section of the BRB. Therefore, it is not suitable for

initiating energy consumption. In a determined structural system, the utilization of a lower steel yield point in the energy dissipation section enables the BRB to achieve yield energy dissipation at an earlier stage, thereby serving as a more effective first line of defense before the main frame yields.

The relationship between length of the BRB energy dissipation section and structure type, structure selection, and material properties determine the maximum proportion. By controlling the length proportion of the energy dissipation section during product design, the desired yield energy consumption can be achieved under different levels of earthquakes. Additionally, the design should meet the ductility safety reserve requirements during rare earthquakes.

References

1. ANSI/AISC 341-02, 2002, *Seismic Provisions for Structural Steel Buildings*, American Institute of Steel Construction, Inc., Chicago, IL
2. ANSI/AISC 341-10, 2010, *Seismic Provisions for Structural Steel Buildings*, American Institute of Steel Construction, Inc., Chicago, IL
3. Benavent-Climent A., Oliver-Saiz E., Donaire-Avila J., 2015, New connection between reinforced concrete building frames and concentric braces: Shaking table tests, *Engineering Structures*, **96**, 7-21
4. Berman J.W., Bruneau M., 2009, Cyclic testing of a buckling restrained braced frame with unconstrained gusset connections, *Journal of Structural Engineering*, **135**, 12, 1499-1510
5. Black C., Makris N., Aiken I., 2002, Component testing, stability analysis and characterization of buckling-restrained unbonded braces, *PEER Report 2002/08*, Pacific Earthquake Engineering Research Center, University of California, Berkeley
6. Cai K.-Q., Huang Y.-Z., Wong C.-X., 2005, Seismic performance and applications of double-tube buckling-restrained braces (in Chinese), *Progress in Steel Building Structures*, **7**, 3, 1-8
7. Di Sarno L., Manfredi G., 2010, Seismic retrofitting with buckling restrained braces: Application to an existing non-ductile RC framed building, *Soil Dynamics and Earthquake Engineering*, **30**, 11, 1279-1297
8. Fan C., Bao X., Hao J., Zhang H., Zhong W., Zhang K., 2021, Performance-based aseismic design method for diamond grid braced frame structure (in Chinese), *Journal of Vibration and Shock*, **40**, 23, 143-151
9. FEMA356, 2000, FEMA, *Prestandard and Commmentary for the Seismic Rehabilitation of Buildings*, Federal Emergency Management Agency, Washington, D.C.
10. GB50011-2010, 2010, *Code for Seismic Design of Buildings*, Ministry of Housing and Urban-Rural Development of the People's Republic of China, Beijing
11. Iwata M., Murai M., 2006, Buckling-restrained brace using steel mortar planks; performance evaluation as a hysteretic damper, *Earthquake Engineering and Structural Dynamics*, **35**, 14, 1807-1826
12. Khampanit A., Leelataviwat S., Kochanin J., Warnitchai P., 2014, Energy-based seismic strengthening design of non-ductile reinforced concrete frames using buckling-restrained braces, *Engineering Structures*, **81**, 110-122
13. Kurata M., Sato M., Zhang L., Lavan O., Becker T., Nakashima M., 2016, Minimal-disturbance seismic rehabilitation of steel moment-resisting frames using light-weight steel elements, *Earthquake Engineering and Structural Dynamics*, **45**, 3, 383-400
14. Li G., Sun F., Zhang Y., 2010, Application classification standard and performance standard of buckling restrained brace (in Chinese), *Journal of Civil, Architectural and Environmental Engineering*, **33**, 2, 391-396

15. Lin P.C., Tsai K.C., Wu A.C., Chuang M.C., 2014, Seismic design and test of gusset connections for buckling-restrained braced frames, *Earthquake Engineering and Structural Dynamics*, **43**, 4, 565-587

16. Maheri M.R., Ghaffarzadeh H., 2008, Connection overstrength in steel-braced RC frames, *Engineering Structures*, **30**, 7, 1938-1948

17. Qu Z., Kishiki S., Maida Y., Sakata H., Wada A., 2015, Seismic responses of reinforced concrete frames with buckling restrained braces in zigzag configuration, *Engineering Structures*, **105**, 12-21

18. Qu Z., Kishiki S., Sakata H., Wada A., Maida Y., 2013, Subassemblage cyclic loading test of RC frame with buckling restrained braces in zigzag configuration, *Earthquake Engineering and Structural Dynamics*, **42**, 7, 1087-1102

19. Qu Z., Xie J., Wang T., Kishiki S., 2017, Cyclic loading test of double K-braced reinforced concrete frame subassemblies with buckling restrained braces, *Engineering Structures*, **139**, 1-14

20. Sabelli R., Roeder C.W., Hajjar J.F., 2013, Seismic design of steel special concentrically braced frame systems: A guide for practising engineers, *NEHRP Seismic Design Technical Brief*, **8**, National Institute of Standards and Technology, USA

21. T/CECS 817-2021, 2021, *Technical Specification for Application of Buckling Restrained Brace*, China Association for Engineering Construction Standardization, Beijing

22. Wakabayashi M., Nakamura T., Katagihara A., 1973, Experimental study on the elasto-plastic behavior of braces enclosed by precast concrete panels under horizontal cyclic loading, *Technical Papers of Annual Meeting*, Architectural Institute of Japan, Tokyo, 1041-1044

23. Wu K., Tao Z., Yu W., Lan X., Zhang L., 2021, Discussion on the parameters matching of a buckling restrained brace in structural design (in Chinese), *Journal of Vibration and Shock*, **40**, 14, 117-124

24. Xie J., 2016, *Seismic Performance Research of Double K-braced Reinforced Concrete Frame with Buckling Restrained Braces*, Master's Thesis, Institute of Engineering Mechanics, China Earthquake Administration, Harbin

25. Yoshino T., Karino Y., 1971, Experimental study on shear wall with braces, Part 2, *Technical Papers of Annual Meeting*, Architectural Institute of Japan, Tokyo, 403-404

Manuscript received February 1, 2024; accepted for publication October 7, 2024